

29P/Schwassmann-Wachmann 1, A Centaur in the Gateway to the Jupiter-Family Comets

G. SARID,¹ K. VOLK,² J.K. STECKLOFF,^{3,4} W. HARRIS,² M. WOMACK,¹ AND L.M. WOODNEY⁵

¹*University of Central Florida, Florida Space Institute*

²*Lunar and Planetary Laboratory, The University of Arizona*

³*Planetary Science Institute*

⁴*University of Texas at Austin, Department of Aerospace Engineering and Engineering Mechanics*

⁵*California State University San Bernardino, Department of Physics*

ABSTRACT

Jupiter Family Comets (JFCs) are the evolutionary products of trans-Neptunian objects (TNOs) that evolve through the giant planet region as Centaurs and into the inner solar system. Through numerical orbital evolution calculations following a large number of TNO test particles that enter the Centaur population, we have identified a short-lived dynamical Gateway, a temporary low-eccentricity orbit exterior to Jupiter through which the majority of Centaurs that become JFCs pass. We apply an observationally-derived size distribution function to our modeled Centaur population and an empirical fading law to our simulated JFCs to estimate the population in this Gateway region; this produces results that are consistent with the observed number of objects in the Gateway. Currently, the most notable occupant of the Gateway region is Centaur 29P/Schwassmann-Wachmann 1 (SW1), a highly active, regularly outbursting Centaur; its present-day, very low eccentricity orbit was established after a 1975 Jupiter conjunction and will continue until a 2038 Jupiter conjunction doubles its eccentricity and pushes its semi-major axis out to its current aphelion. Within the next 10,000 years, SW1 will likely evolve out of the Gateway region to become the largest JFC. The JFC Gateway region coincides with a heliocentric distance range where the activity of all observed cometary bodies increases significantly, so SW1's activity may be typical of the early evolutionary processing experienced by most JFCs. Thus, the Gateway region, and its most notable occupant SW1, are critical to both the dynamical and physical transition between Centaurs and JFCs.

1. INTRODUCTION

Centaurs are a transient population of icy bodies that represent the link between the outer solar system's trans-Neptunian object (TNO) population and the Jupiter Family Comets (JFCs). Centaurs have perihelia and semi-major axes between the orbits of Jupiter and Neptune (Jewitt 2009), so their dynamical evolution is driven by frequent gravitational perturbations from the giant planets. JFCs are comets whose dynamics are controlled by Jupiter; they are often defined using the Tisserand parameter with respect to Jupiter ($T_J = a_J/a + 2\sqrt{a/a_j(1 - e^2)} \cos i$) to have $2 < T_J < 3$. Because

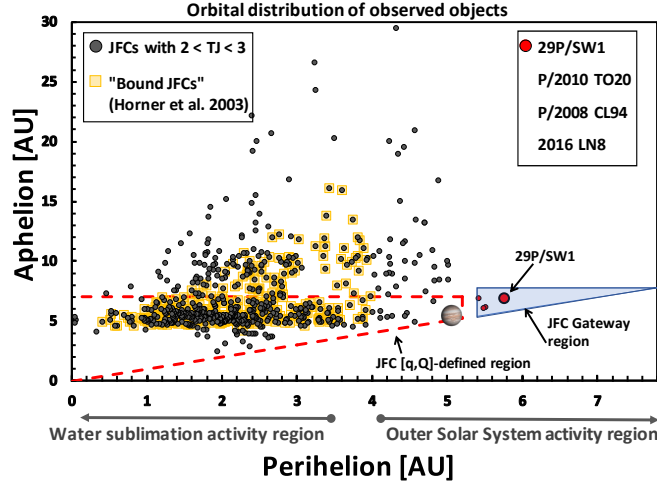


Figure 1. Perihelion-aphelion distribution of JFCs (gray circles; $2 < T_J < 3$) and several objects of interest, including SW1 (red circles). Our $[q,Q]$ -defined JFC population is enclosed by the dashed red line. The “JFC Gateway region” is shown in blue (see Section 2). A Tisserand parameter-based classification of “bound JFCs” (Horner et al. 2003) is shown for comparison (yellow squares). We note a distinction in the main mechanisms driving activity using gray arrows along the x-axis: the water ice sublimation controlled region extends inward from ~ 3.5 au and mechanisms other than water sublimation are prominent from ~ 4 au outward.

the Tisserand parameter neglects the presence of the other planets, we use a second definition of Jupiter-controlled JFCs: objects with perihelia interior to Jupiter ($q < 5.2$ au) and aphelia well separated from Saturn ($Q < 7$ au); we refer to this as our $[q-Q]$ definition.

Fig. 1 illustrates the JFC population defined using T_J and $[q-Q]$. For reference, we include another dynamical mapping of JFCs that divides objects with $T_J < 3$ into several dynamical groups (e.g., ‘loosely bound’ $2.5 < T_J < 2.8$ and ‘tightly bound’ $2.8 < T_J < 3$), all with $q < 4$ au (Horner et al. 2003). Our $[q-Q]$ -defined JFCs include $\sim 75\%$ of those ‘bound’ objects while also including some objects with $q > 4$ that may be transitioning to JFC status.

Centaur evolution is dominated by chaotic gravitational perturbations, so an individual Centaur’s orbital pathway through the giant planet region is highly sensitive to its initial conditions. Nevertheless, trends emerge in the evolution of Centaurs as a whole. Passage through the Centaur region typically take $\sim 1 - 10$ Myr (Tiscareno & Malhotra 2003; Duncan et al. 2004; Di Sisto & Brunini 2007), with multiple possible outcomes. The giant planets can eject Centaurs back into the TNO’s scattering population, into the Oort Cloud, or out of the solar system entirely (see, e.g., Dones et al. 2015). Centaurs that evolve inward into the JFC population avoid such ejection, passing through many gravitational interactions and, conceivably, a gateway transition region to enter (or exit) the inner solar system. A total Centaur population of order 10^7 objects larger than 2 km in diameter is consistent with the prevalence of small nuclei in the JFC population (Sheppard et al. 2000).

29P/Schwassmann-Wachmann 1 (hereafter SW1), discovered while outbursting in 1927, was the first observed small body with an orbit entirely beyond Jupiter. While its activity/outburst characteristics led to its classification as a comet, the subsequent discovery of other bodies between Jupiter and Neptune, followed by dynamical models linking TNOs and JFCs, place SW1 in better context as a member of the Centaur population. SW1’s low-inclination ($i = 9.37^\circ$) and nearly circular orbit (heliocentric distance range 5.77-6.28 au; $e = 0.043$) put it at the inner edge of the Centaur region;

its Tisserand parameter ($T_J = 2.985$) also places it at the cusp between the two populations (e.g. Fernández et al. 2018).

While initially SW1 appears to be an outlier, there are three other observed objects in its orbital region: P/2010 TO20 LINEAR-Grauer, P/2008 CL94 Lemmon and 2016 LN8. Fig. 1 shows these objects, highlighting their position relative to the JFCs. Their sizes, estimated from photometric observations or H-magnitudes (assuming an albedo of 0.1), are between 4 – 12 km (Lacerda 2013; Kulyk et al. 2016). While these objects meet the orbital definition of a Centaur, they also have T_J near the upper boundary of the JFC definition (with 2016 LN8’s T_J in the middle of the JFC range due to its inclination of 43°). Interestingly, in 2011, P/2010 TO20 had an orbit confined between 5.1-6.1 au, compared with its current orbit spanning 5.5-6.1 au; this short-timescale variation underscores the transient nature of this Gateway region between Centaurs and JFCs (see definition of “JFC Gateway Region” in Sec. 2).

SW1 is the only known large active Centaur in the Gateway region. Additionally, it is the only icy object with a predictable pattern of major outbursts (Trigo-Rodríguez et al. 2008; Miles et al. 2016), despite its orbit being entirely beyond the region where surface water-ice sublimates efficiently (distances $\lesssim 4 - 5$ au). However, the Gateway region where SW1 resides (heliocentric distances of $\sim 5 - 7$ au) is where many distantly active comets show strong increases in out-gassing and outbursts. One of the leading mechanisms proposed for driving this activity is the rapid crystallization of amorphous water ice (e.g. Sarid & Prialnik 2009; Womack et al. 2017). Newly exposed volatile ice patches (e.g., CO, CO₂) or release of sub-surface volatile gas pockets are also proposed distant-activity mechanisms (see, e.g. Prialnik et al. 2004; Guilbert-Lepoutre et al. 2015). Indeed, CO gas has been measured in SW1’s coma during all activity phases, even sometimes exceeding CO production rates of comet C/1995 O1 (Hale-Bopp) at SW1’s heliocentric distance (Womack et al. 2017).

It may be the case that the Gateway region, with its potentially overlapping activity mechanisms, is where inbound JFCs experience the onset of a bona-fide cometary activity. SW1’s orbital configuration and unique activity characteristics motivate us to examine its orbital context and its relationship to the other prominent group of active objects, the JFCs.

2. DYNAMICAL MODELING OF THE TNO-CENTAUR-JFC TRANSITION

We take a forward modeling approach to determine how objects evolve dynamically from TNO reservoirs, through the Centaur population, and into the JFC region. The latter transition involves a relatively transient, yet robust, phase of SW1-like orbits, which we call the “JFC Gateway region”.

To account for vastly differing timescales in different regions of the solar system, we model this in two parts: 1) the dynamical evolution of the TNO source population into the Centaur population ($\sim 10^8 - 10^9$ yrs) and 2) detailed evolution of Centaur orbits ($\sim 10^6 - 10^7$ yrs), their passage through the JFC Gateway region, and subsequent evolution as JFCs ($\sim 10^4 - 10^5$ yrs). The first part can be modeled with only gravitational perturbations from the Sun and giant planets, greatly reducing the computational cost of long-timescale simulations; the second part requires including the terrestrial planets and thus a much smaller integration time-step.

To model Centaur production, we integrate test particles representing TNO populations forward in time for 500 Myr under the gravitational influence of the Sun and four giant planets. We use the Mercurius package within the REBOUND orbit integration software package (Rein & Liu 2012) which allows us to track particles through close encounters with the planets. We follow each test particle until it reaches heliocentric distances either greater than 2000 au or less than 4 au. The

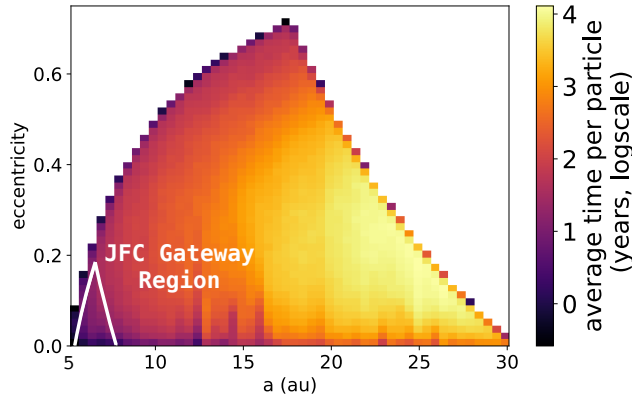


Figure 2. Average time spent (log scale; in color) per Centaur test particle at different semimajor axes and eccentricities; note that not all particles that become Centaurs evolve to small semimajor axes, so the time distribution reflects both local dynamical timescales and the probability of a particle arriving at that $a - e$ combination. The white lines indicate the boundaries of our JFC Gateway region.

inner boundary is set by the absence of the terrestrial planets, while the outer boundary is set by the absence of galactic tides and other external influences that become important far from the Sun. As test particles enter the Centaur population (which here we define as orbits entirely contained in the giant planet region; $q > 5.2$ au and $Q < 30.1$ au), we record their orbital history at a high cadence, allowing us to produce high resolution maps of their ensemble orbital evolution.

We consider two different TNO source region models for these integrations to test whether the distribution of Centaurs (and the nature of the Centaur to JFC transition) depends on the assumed source region distribution. We model: 1) the actively scattering trans-Neptunian population and 2) a simplified “stirred” classical Kuiper belt population. The actively scattering objects have orbits which are currently evolving in semi-major axis due to perturbations from the giant planets (Gladman et al. 2008). We use a scattering population model from Kaib et al. (2011) as our initial conditions, which is consistent with current observations of the outer solar system (Shankman et al. 2016; Lawler et al. 2018). This model extends to the inner Oort cloud, so we take only orbits with semi-major axes smaller than 1000 au. We start with ~ 17000 test particles, of which ~ 1100 enter the Centaur population within 500 Myr.

For the classical Kuiper belt, we model the “stirred” population: objects confined to semi-major axes $a = 42 - 47$ au with perihelia $q > 37$ au (Petit et al. 2011). We assume a Rayleigh distribution of inclinations with a width of 5° (for comparison, the model scattering population’s width is $\sim 15^\circ$). We find that ~ 2300 of our initial ~ 25000 stirred classical belt particles enter the Centaur region within 500 Myr ¹.

As expected, highly chaotic evolution in the giant planet region largely erases these Centaurs’ initial TNO conditions. Fig. 2 shows the time-weighted distribution of particles in the Centaur region (we combined both simulations because there are no significant differences in the $a - e$ distribution). The median time these test particles spend with orbits entirely within the giant planet region is

¹ Note that this does not reflect the current classical belt’s absolute Centaur production rate because these simplified initial conditions include unstable regions of resonances with Neptune that overlap the classical belt population.

~ 2.4 Myr, the majority of which is spent in the outer Centaur region; approximately 80% and 50% of Centaur test particles reach semi-major axes interior to Uranus and Saturn, respectively.

We define the ‘‘JFC Gateway region’’ as containing orbits with relatively low eccentricity that are not Jupiter crossing and have aphelia well-separated from Saturn: $q > 5.4$ au (perihelion outside Jupiter’s aphelion) and $Q < 7.8$ au (aphelion > 4 Hill radii away from Saturn’s semi-major axis and $\gtrsim 3$ Hill radii from Saturn’s perihelion). Our simulations produced ~ 3200 Centaurs within 500 Myr, and ~ 700 (21%) of these particles spend time in this JFC Gateway region. Note that this percentage and the total time these Centaurs spend in the JFC Gateway region (Fig. 2) reflects only evolution prior to entering the inner solar system due to the absence of the terrestrial planets in these initial simulations.

To explore the transition between the Centaurs and JFCs (which requires including the terrestrial planets in the simulations), we took as initial conditions the orbit of every Centaur test particle from the above simulations at the time-step that it first reached semi-major axis $a < 30$ au. These orbits were each cloned 10 times by randomizing mean anomalies, longitudes of ascending node, and arguments of perihelion and then integrated forward using Mercurius under the influence of the Sun, the terrestrial planets, and the giant planets for 10^8 years. Test particles were removed if they came too close to the Sun ($q < 0.05$ au) or were ejected to very distant ($Q > 2000$ au) orbits. Orbital histories for the test particles were output at increasingly frequent intervals as they moved to smaller semi-major axes (ranging from every 5000 years near Neptune to every 5 years in the inner solar system). As noted earlier, the evolution of test particles in the inner solar system does not strongly depend on the particular TNO distribution, so we combine both source regions in our analysis, giving us a sample size of nearly 12000 JFC test particles.

3. RESULTS AND IMPLICATIONS

Table 1 summarizes our simulation results for the transition between the Centaurs and the JFCs including how many JFC test particles spend time in the JFC Gateway region, their median and average residency time there, and the relative timing of Gateway occupancy. Accounting for only gravitational evolution (we consider the effects of fading in Sec. 3.1), we find that 72% of all JFCs spend some time in the Gateway region. The median time spent in this region is 1700 years; nearly half of all JFCs that evolve to $q < 3$ au (where water out-gassing becomes a dominant activity driver) will spend time (median: 700 years) in this Gateway region before reaching these small heliocentric distances. Tracking all test particles that pass through the Gateway, we find that 77% of these particles are classified as JFCs at some point in the simulation. Fig. 3 shows the time-weighted orbital distribution of all our JFC test particles.

3.1. *Evolving back and forth between the Centaurs and JFCs*

Gravitational perturbations can evolve JFC nuclei back into the Centaur population, complicating our characterization of the Gateway region and comparisons between our dynamical study and observations of JFCs and Centaurs. For example, simulations of only the initial Centaur evolution (Sec. 2, Fig. 2), indicate 21% of Centaurs enter the JFC Gateway region. However, in our full simulations of inner and outer solar system orbital evolution (Fig. 3), this increases to $\sim 30\%$.

Some of the test particles in the JFC Gateway region arrive there after being at small heliocentric distances (see Table 1). In the real solar system, this would require comet nuclei to survive the thermal environment of its residency in the inner solar system where surface and near-surface volatile material

Table 1. Summary of simulation results ([q-Q] definition for JFCs)

All test particles			
		no fading	BW15 fading
# JFCs generated		11792	11792
# JFCs passing through JFC Gateway phase		8465	7817
Median time spent in JFC Gateway phase (yrs)		1750	425
Average time spent in JFC Gateway phase (yrs)		8000	1675
Particles having a JFC Gateway phase prior to reaching			
perihelion distance	percentage	t_{median} (yrs)	$t_{average}$ (yrs)
$q < 4$ au	38%	625	4050
$q < 3.5$ au	44%	650	3950
$q < 3$ au	49%	700	3925

NOTE—The ‘no fading’ columns in the top portion of the table reflect purely gravitational evolution in the simulations. The ‘BW15 fading’ column reflects those same simulations with [Brasser & Wang \(2015\)](#)’s empirical fading law applied as a weighting factor for each particle. The bottom portion of the table details the relative timing of the JFC gateway phase. For example, 38% of JFCs visit the Gateway before reaching $q < 4$ au, with a median residence time of 625 years prior to reaching $q < 4$ au.

(e.g. water ice) is heated and can quickly sublimate and trigger mass loss (e.g. [Meech & Svoren 2004](#); [Guilbert-Lepoutre et al. 2015](#)). In addition to sublimation, other mechanisms can affect the physical evolution of comet nuclei, such as: lag deposit insulation that quenches activity (e.g. [Prialnik et al. 2004](#)), sublimative torques that can spin up nuclei and trigger mass wasting or splitting (e.g. [Steckloff & Jacobson 2016](#); [Steckloff & Samarasinha 2018](#)), localized erosion that can induce mass loss or (e.g. [Vincent et al. 2017](#)). Thus, over time nuclei can be removed from the comet population.

We must account for such physical processing in our simulated population statistics. The exact physical evolution for any particular comet is complicated and stochastic. However, the physical processing of an ensemble of objects can be approximated using a “fading law”, which describes the typical behavior of comet nuclei based on fits to observed trends.

There are different ways to construct a JFC fading law, depending on what mechanisms are considered most prominent (e.g. [Chen & Jewitt 1994](#); [Boehnhardt 2004](#); [Samarasinha 2007](#); [Belton 2015](#)). For our purposes, we chose the [Brasser & Wang \(2015\)](#) implementation, which is derived from a large set of dynamical simulations fitted to the observed JFC population. Their best-fit result is a delayed power law that describes how the visibility ϕ_m of a comet is reduced over time as a function of the number of perihelion passages m it experiences with $q < 2.5$ au:

$$\phi_m \propto (M^2 + m^2)^{-k/2}, \quad (1)$$

where $k \sim 1.4$ and $M = 40$. [Brasser & Wang \(2015\)](#)’s analysis included comets with diameters down to 2.3 km. This size limit is sufficient for our purposes, as it is about half the diameter of the smallest known object in the Gateway region (Sec. 1). Comet nuclei size distributions for smaller sizes are currently poorly constrained and incomplete ([Snodgrass et al. 2011](#); [Fernández et al. 2013](#)) and the fragmentation rate at such small sizes is likely very high (see [Belton 2015](#)).

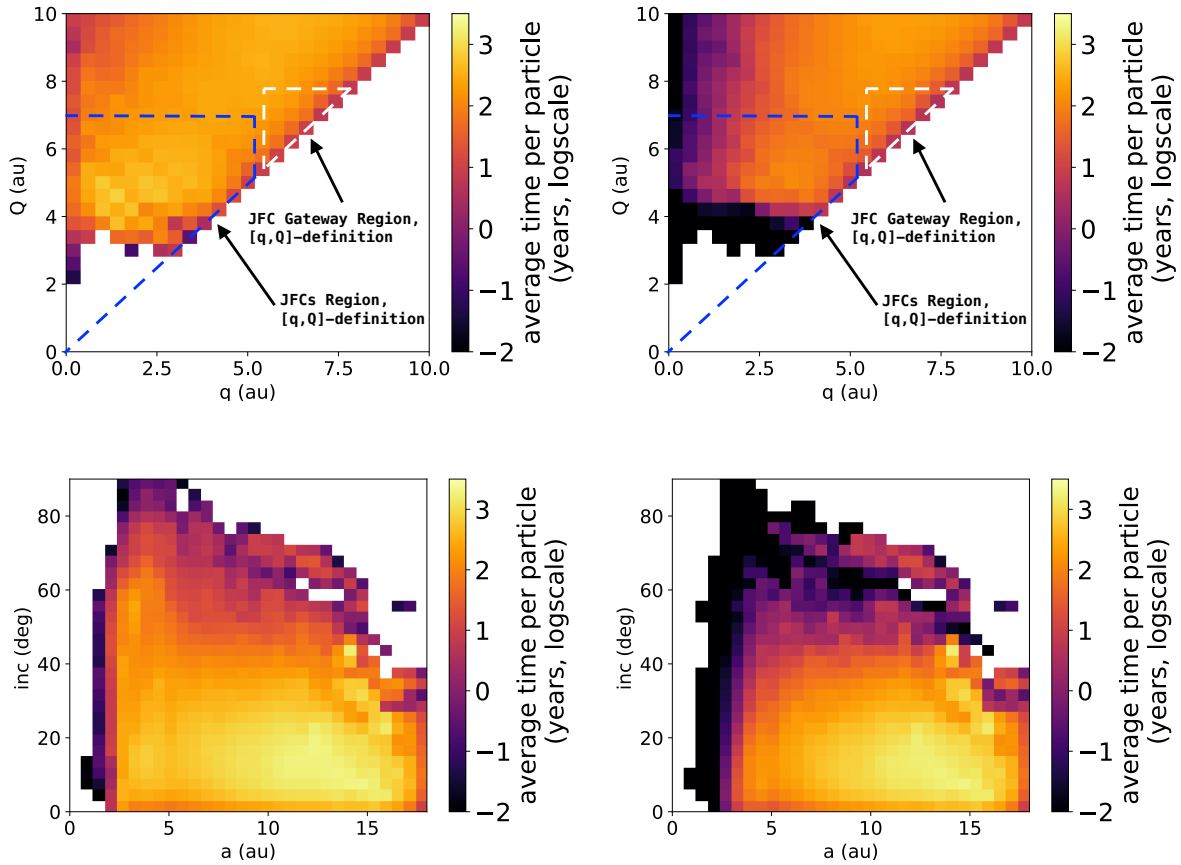


Figure 3. Time-weighted orbital distribution of JFC test particles (using our $[q,Q]$ -JFC definition to select JFCs) from our full simulations. **Left panels:** purely dynamical evolution, no fading law applied. **Right panels:** particles are weighted according to the Brassier & Wang (2015) fading law (Section 3.1). The top panels show aphelion vs. perihelion distributions near the transition between Centaurs and JFCs. The bottom panels show inclination vs. semi-major axis. It is clear that fading decreases the amount of time JFCs spend at small perihelion distances and large inclinations. JFCs that fade also spend less time in the JFC Gateway region because fading limits their ability to re-visit the region after spending time as inner solar system JFCs.

To apply this fading law to our simulations, we use ϕ_m to weight each test particle in the analysis of the time-averaged population. With this fading law, we still find that the majority of JFCs (66%) spend time in the Gateway region. The median total time in the Gateway region drops from 1750 years to 425 years (Table 1), because JFCs reaching low perihelion distances tend to fade before moving back out into this region. Fig. 3 shows the time-weighted distributions of our JFC test particles with and without this fading law. In particular, the inclination vs. semi-major axis distribution highlights why fading laws are typically implemented. Purely dynamical interactions with the planets tend to increase orbital inclinations as test particles spend more time in the inner solar system, making their distribution inconsistent with the lower observed inclinations in the real solar system (see, e.g., Nesvorný et al. 2017); fading limits particle lifetimes and thus limits their inclinations.

3.2. Expected occupancy of the JFC Gateway region

The presence of this Gateway region, through which the majority of JFCs pass, provides a testable connection between the observed JFC and Centaur populations. We can estimate the time-averaged number of objects currently residing in this region beyond Jupiter at different sizes, as a check on the validity of our dynamical model. To do this, we employ a Centaur size distribution function based on the observed cratering record in the Pluto-Charon system (Singer et al. 2019), the observed size distribution function of JFCs with measured radii $r > 4$ km (Snodgrass et al. 2011), and the fragment size fit for C/1999 S4 (LINEAR) following its total breakup (Mäkinen et al. 2001). From these studies, we obtain a power law size distribution for the Centaurs:

$$dN_r = -k\alpha r^{-\alpha+1} dr, \quad (2)$$

where $\alpha = 3$ and $k = 6.5 \times 10^6$; this reasonably reproduces the number of known Centaurs with $r > 50$ km (~ 50 objects in the MPC database in this size range). Integrating over all radii $r > 1$ km, we obtain a total Centaur population of 6.5×10^6 , which is consistent with previous estimates (Sheppard et al. 2000).

The expected time-averaged occupancy of the Gateway region for specific size ranges is obtained by multiplying the integrated size distribution by our derived values of: the percentage of all Centaurs that enter the Gateway region (30%, including JFCs re-entering the Centaur population); the ratio of the median residency time in the Gateway (Table 1, depends on fading) to the median dynamical lifetime in the Centaur region (2.6×10^6 yr, Sec. 2). If we consider the size range of the four objects observed to be in the Gateway ($4 < r < 35$ km), the expected occupancy rate from our model ranges from ~ 5 (with fading) to ~ 20 (without fading) objects, consistent with observations. Objects as large or larger than SW1 (radius estimated to be $25 < r < 35$ km; Schambeau et al. 2017) are significantly less likely, with an expected occupancy rate ranging from 0.02 (with fading) to 0.085 (without fading). That makes large objects in the Gateway region rare enough on the $\sim 10^4$ year timescale of human civilization that SW1 is likely the first such object to enter the Gateway in recorded history.

An interesting prediction from our model is the large expected occupancy rate in the Gateway region for Centaurs with $r > 1$ km, ranging from ~ 300 (with fading) to ~ 1000 (without fading). Such a large instantaneous population would experience very close encounters with Jupiter. This may explain the impact frequency of events such as Shoemaker-Levy 9 (1993) and the later, serendipitous impact detection in 2009 (Sánchez-Lavega et al. 2010; Hueso et al. 2013).

3.3. Implications for SW1

SW1 falls into the category of objects that are large enough to be relatively unaffected by physical fading mechanisms (e.g. Belton 2015). These larger objects are thus more likely than small objects to revisit the Gateway region after spending time at low perihelion distances. Here we discuss SW1's activity characteristics and likely orbital history in this context.

Due to its close proximity to Jupiter, SW1's orbit evolves significantly on short timescales. Fig. 4 shows the recent past and near future evolution of SW1. ² Currently, SW1's orbit undergoes semi-major axis and eccentricity changes when it comes to conjunction with Jupiter every ~ 50 years. Its present-day, very low eccentricity orbit ($e = 0.043$) was established after a 1975 conjunction and will

² We take the Jan 2010 orbit fit and uncertainties from JPL Horizons (Giorgini et al. 1996) as our initial conditions.

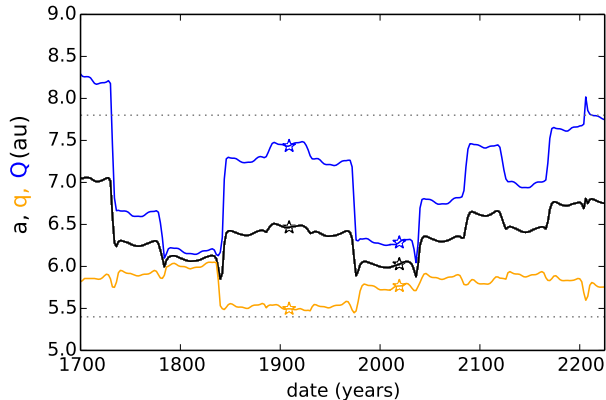


Figure 4. Short-term orbital evolution (in semimajor axis a , perihelion q , and aphelion Q) of SW1. The dashed horizontal lines denote our JFC Gateway region. SW1’s orbit significantly changed due to a Jupiter conjunction in 1975, and it will change again soon in 2038 due to another conjunction with Jupiter. The stars show SW1’s observed orbits in 2019 and in 1908.

continue until a 2038 Jupiter conjunction nearly doubles its eccentricity and pushes its semi-major axis out to its current aphelion, causing SW1 to experience much wider variations in solar heating. It will be interesting to see whether this new orbit affects its level of activity and cycle of outbursts.

As Fig. 4 shows, the backwards integrations reproduce SW1’s observed orbit more than 100 years ago,³ providing a lower-bound on how long from the present epoch the integrations (which neglect non-gravitational forces) reliably predict SW1’s orbit. Integration of many clones of SW1 (within its orbital uncertainties) indicate that SW1 can be tracked back approximately ~ 700 years before the clones diverge as a result of chaos and a particularly strong Jupiter encounter.

From these calculations, we can only conclusively say that SW1 has spent at least a few hundred years in the JFC Gateway region. We note that SW1’s current low inclination ($\sim 10^\circ$) is suggestive of it not having spent significant time in the inner solar system (see left panels of Fig. 3). SW1’s clones can be integrated forward for several hundred years before their evolution diverges. Further in the future we have only a statistical description of SW1’s evolution: in the next 10^4 years, it has a $\sim 65\%$ chance of becoming a JFC (using our $[q-Q]$ -definition).

We note that based on SW1’s size and activity pattern (somewhat similar to Hale-Bopp, see Womack et al. 2017; Wierzos et al. 2017), were it to enter the JFC population it would be the largest short-period comet ever recorded and most likely the brightest short- or long-period comet ever seen. We have no historical record of such an apparition and no object close to SW1’s size is recorded in the observed short- or long-period comet populations. This implies that Centaur-to-JFC transitions in this size range are rare on the timescale of human civilization and occur with a frequency smaller than the dynamical lifetime of the typical JFC. Interestingly, our dynamical model (Table 1; Section 3.2) supports this conclusion, without setting SW1’s observability or active state as imposed constraints.

Thus, while the exact long-term orbital history of SW1 is unknown, we conclude that SW1’s currently low inclination ($< 10^\circ$), high activity levels comparable to dynamically new long period comets at the same heliocentric distance, and the lack of a historical record of a short period ‘super-

³ The minor planet center orbit fit for the epoch 1908-10-26.

comet’, are more consistent with SW1 being a new visitor to the JFC Gateway rather than a return visitor that had ever spent significant time in the inner solar system.

4. CONCLUSIONS

Our dynamical study of the transition between Centaurs and JFCs, motivated by the intriguing properties of SW1, enabled us to identify and characterize an important orbital niche – a Gateway to/from the JFC population. This region of low-eccentricity orbits just exterior to Jupiter ($q > 5.4$ au, $Q < 7.8$ au) is currently populated by 4 known objects, of which SW1 is the most prominent in terms of size, activity, and observational record.

Our dynamical models reveal that the vast majority of objects (77%) in this Gateway region will become or have already been JFCs, and the majority of JFCs (66-72%, depending on fading) pass through this Gateway. Approximately half of all JFCs will pass through this Gateway region before experiencing significant water-driven sublimation ($q < 3$ au).

The dynamical importance of the JFC Gateway region in which SW1 resides places its activity behavior in much clearer context as a transition between other kinds of active objects in the outer solar system. This can serve as a complimentary dynamical framework for studies of outer solar system activity and surface color distributions (e.g. Jewitt 2009, 2015). In this context, SW1’s active state, likely driven by a non-water-ice sublimation process, is probably typical of the early significant evolutionary processing of objects that subsequently become JFCs.

Our identified Gateway region is an important, albeit brief, stage of orbital, and thus likely physical, evolution that appears exceptionally common for Centaurs to pass through. It deserves additional studies in both modeling and observational capacities to better understand the physical processing of nuclei surfaces and sub-surfaces as objects transition in and out of the Gateway region and better constrain the number and size of such objects. While the pathway SW1 is taking is very common, its short-lived nature means it is rare for an object as large as SW1 to be present at any given epoch. This adds to the motivation for studies of SW1 in particular.

An allocation of computer time from the UA Research Computing High Performance Computing (HPC) at the University of Arizona is gratefully acknowledged. GS acknowledges support from NSF grant 1615917 and NASA award 80NSSC18K0497. KV acknowledges support from NASA grants NNX15AH59G and 80NSSC19K0785 and NSF grant AST-1824869. JS acknowledges support from NSF grant 1910275 and NASA award 80NSSC18K0497. MW acknowledge support from NSF grant 1615917.

REFERENCES

- Belton, M. J. S. 2015, *Icarus*, 245, 87
- Boehnhardt, H. 2004, *Split comets*, ed. M. C. Festou, H. U. Keller, & H. A. Weaver, 301–316
- Brasser, R., & Wang, J. H. 2015, *A&A*, 573, A102
- Chen, J., & Jewitt, D. 1994, *Icarus*, 108, 265
- Di Sisto, R. P., & Brunini, A. 2007, *Icarus*, 190, 224
- Dones, L., Brasser, Ramon, K. N., & Rickman, H. 2015, *SSRv*, 197, 191
- Duncan, M., Levison, H., & Dones, L. 2004, *Dynamical evolution of ecliptic comets*, ed. M. C. Festou, H. U. Keller, & H. A. Weaver, 193
- Fernández, J. A., Helal, M., & Gallardo, T. 2018, *Planet. Space Sci.*, 158, 6
- Fernández, Y. R., Kelley, M. S., Lamy, P. L., et al. 2013, *Icarus*, 226, 1138

- Giorgini, J. D., Yeomans, D. K., Chamberlin, A. B., et al. 1996, in *Bulletin of the American Astronomical Society*, Vol. 28, *Bulletin of the American Astronomical Society*, 1158
- Gladman, B., Marsden, B. G., & Van Laerhoven, C. 2008, in *The Solar System Beyond Neptune*, ed. M. A. Barucci, H. Boehnhardt, D. P. Cruikshank, A. Morbidelli, & R. Dotson (The University of Arizona Press), 43–57
- Guilbert-Lepoutre, A., Besse, S., Mousis, O., et al. 2015, *SSRv*, 197, 271
- Horner, J., Evans, N. W., Bailey, M. E., & Asher, D. J. 2003, *MNRAS*, 343, 1057
- Hueso, R., Pérez-Hoyos, S., Sánchez-Lavega, A., et al. 2013, *A&A*, 560, A55
- Jewitt, D. 2009, *AJ*, 137, 4296
- . 2015, *AJ*, 150, 201
- Kaib, N. A., Roškar, R., & Quinn, T. 2011, *Icarus*, 215, 491
- Kulyk, I., Korsun, P., Rousselot, P., Afanasiev, V., & Ivanova, O. 2016, *Icarus*, 271, 314
- Lacerda, P. 2013, *MNRAS*, 428, 1818
- Lawler, S. M., Shankman, C., Kavelaars, J. J., et al. 2018, *AJ*, 155, 197
- Mäkinen, J. T. T., Bertaux, J.-L., Combi, M. R., & Quémerais, E. 2001, *Science*, 292, 1326
- Meech, K. J., & Svoren, J. 2004, *Using cometary activity to trace the physical and chemical evolution of cometary nuclei*, ed. M. C. Festou, H. U. Keller, & H. A. Weaver, 317
- Miles, R., Faillace, G. A., Mottola, S., et al. 2016, *Icarus*, 272, 327
- Nesvorný, D., Vokrouhlický, D., Dones, L., et al. 2017, *ApJ*, 845, 27
- Petit, J.-M., Kavelaars, J. J., Gladman, B. J., et al. 2011, *AJ*, 142, 131
- Prialnik, D., Benkhoff, J., & Podolak, M. 2004, *Modeling the structure and activity of comet nuclei*, ed. M. C. Festou, H. U. Keller, & H. A. Weaver, 359
- Rein, H., & Liu, S.-F. 2012, *A&A*, 537, A128
- Samarasinha, N. H. 2007, *Advances in Space Research*, 39, 421
- Sánchez-Lavega, A., Wesley, A., Orton, G., et al. 2010, *ApJL*, 715, L155
- Sarid, G., & Prialnik, D. 2009, *Meteoritics and Planetary Science*, 44, 1905
- Schambeau, C. A., Fernández, Y. R., Samarasinha, N. H., Mueller, B. E. A., & Woodney, L. M. 2017, *Icarus*, 284, 359
- Shankman, C., Kavelaars, J., Gladman, B. J., et al. 2016, *AJ*, 151, 31
- Sheppard, S. S., Jewitt, D. C., Trujillo, C. A., Brown, M. J. I., & Ashley, M. C. B. 2000, *AJ*, 120, 2687
- Singer, K. N., McKinnon, W. B., Gladman, B., et al. 2019, *Science*, 363, 955
- Snodgrass, C., Fitzsimmons, A., Lowry, S. C., & Weissman, P. 2011, *MNRAS*, 414, 458
- Steckloff, J. K., & Jacobson, S. A. 2016, *Icarus*, 264, 160
- Steckloff, J. K., & Samarasinha, N. H. 2018, *Icarus*, 312, 172
- Tiscareno, M. S., & Malhotra, R. 2003, *AJ*, 126, 3122
- Trigo-Rodríguez, J. M., García-Melendo, E., Davidsson, B. J. R., et al. 2008, *A&A*, 485, 599
- Vincent, J. B., Hviid, S. F., Mottola, S., et al. 2017, *MNRAS*, 469, S329
- Wierzchos, K., Womack, M., & Sarid, G. 2017, *AJ*, 153, 230
- Womack, M., Sarid, G., & Wierzchos, K. 2017, *PASP*, 129, 031001